PCCP

View Online
Dynamic Article Links

Cite this: *Phys. Chem. Chem. Phys.*, 2011, **13**, 15865–15872

www.rsc.org/pccp

PAPER

Microscopic solvation of $NaBO_2$ in water: anion photoelectron spectroscopy and *ab initio* calculations†

Yuan Feng, Min Cheng, Xiang-Yu Kong, Hong-Guang Xu and Wei-Jun Zheng*

Received 20th March 2011, Accepted 17th June 2011
DOI: 10.1039/c1cp20831d

We investigated the microscopic solvation of $NaBO_2$ in water by conducting photoelectron spectroscopy and *ab initio* studies on $NaBO_2^-(H_2O)_n$ (n = 0–4) clusters. The vertical detachment energy (VDE) of $NaBO_2^-$ is estimated to be 1.00 ± 0.08 eV. The photoelectron spectra of $NaBO_2^-(H_2O)_1$ and $NaBO_2^-(H_2O)_2$ are similar to that of bare $NaBO_2^-$, except that their VDEs shift to higher electron binding energies (EBE). For the spectra of $NaBO_2^-(H_2O)_3$ and $NaBO_2^-(H_2O)_4$, a low EBE feature appears dramatically in addition to the features observed in the spectra of $NaBO_2^-(H_2O)_{0-2}$. Our study shows that the water molecules mainly interact with the BO_2^- unit in $NaBO_2^-(H_2O)_1$ and $NaBO_2^-(H_2O)_2$ clusters to form Na–$BO_2^-(H_2O)_n$ type structures, while in $NaBO_2^-(H_2O)_3$ and $NaBO_2^-(H_2O)_4$ clusters, the water molecules can interact strongly with the Na atom, therefore, the Na–$BO_2^-(H_2O)_n$ and $Na(H_2O)_n\cdots BO_2^-$ types of structures coexist. That can be seen as an initial step of the transition from a contact ion pair (CIP) structure to a solvent-separated ion pair (SSIP) structure for the dissolution of $NaBO_2$.

1. Introduction

Dissolved salts play important roles in inorganic and organic reactions, biochemistry,[1–3] marine chemistry,[4] atmospheric chemistry,[5–8] and our daily life.[9,10] Dissolution of salts is a very fundamental process in chemistry. Therefore, many theoretical[11–22] and experimental[23–31] works have been conducted to investigate the microscopic mechanisms of salt dissolution. The previous theoretical and experimental efforts are mainly focused on alkali halide salts since they are the simplest and most common salts. It has been suggested[32] that a salt molecule may first exist as a contact ion pair (CIP) in which the anion and cation interact with each other directly with no interference from the solvent molecules. During the solvation process, the anion and cation in the salt molecule can be separated by the solvent molecules to form a solvent-separated ion pair (SSIP). One interesting question is how many solvent molecules are needed in order to separate the contact ion pair of a particular salt molecule.[16] As the ionic bonds of salts can be significantly affected by the solvent molecules, it is expected that the electron state of a SSIP would be different from that of a CIP. Thus, a good approach for studying the evolution of a salt CIP structure to a SSIP structure in the solvation processes is to probe the change in the salt electronic state with an increasing number of solvent molecules using anion photoelectron spectroscopy. Wang and coworkers have investigated $[M^+(SO_4^{2-})]_{1-2}$ (M = Na, K) ion pairs[27] and dissolution of $NaSO_4^-$ by water[33] using anion photoelectron spectroscopy. However, there is no photoelectron spectroscopy study of the other salt–water complexes yet. Since sodium metaborate ($NaBO_2$) and its hydrate are key materials in the recycling process of $NaBH_4$ for hydrogen storage and generation,[34] understanding the solvation process of $NaBO_2$ is important from both technological and scientific points of view. Recent photoelectron spectroscopy and theoretical studies of $Fe_nBO_2^-$ (n = 1–10),[35] $Au_n(BO_2)_m^-$,[36,37] and $Cu_n(BO_2)_m^-$[38] clusters confirmed the theoretical prediction[39] that BO_2 can be considered as a superhalogen. $NaBO_2$ may be viewed as a superhalogen salt in the form of $Na^+(BO_2)^-$, which is analogous to the alkali halides. Thus, investigation of $NaBO_2^-(H_2O)_n$ might also be helpful for understanding the solvation of alkali halides. In this work, we investigate the microscopic solvation of $NaBO_2$ in water *via* anion photoelectron spectroscopy and *ab initio* calculations of $NaBO_2^-(H_2O)_n$ clusters. Our study shows that there is a significant change in the photoelectron spectra of $NaBO_2^-(H_2O)_n$ clusters starting from n = 3. That is evidence of solvent separation of Na and $(OBO)^-$ units.

2. Experimental and computational methods

2.1 Experimental

The experiments were conducted with a home-built apparatus consisting of a time-of-flight mass spectrometer and a

Beijing National Laboratory for Molecular Sciences, State Key Laboratory of Molecular Reaction Dynamics, Institute of Chemistry, Chinese Academy of Sciences, Beijing 100190, China. E-mail: zhengwj@iccas.ac.cn; Fax: +86 10 62563167; Tel: +86 10 62635054

† Electronic supplementary information (ESI) available. See DOI: 10.1039/c1cp20831d

magnetic-bottle photoelectron spectrometer, which has been described elsewhere.[40] Briefly, the $NaBO_2^-(H_2O)_n$ cluster anions were produced in a laser vaporization source by ablating a rotating, translating sodium tetraborate target with the second harmonic (532 nm) light pulses of a Nd:YAG laser, while helium carrier gas with 4 atm backing pressure seeded with water vapor was allowed to expand through a pulsed valve for generating hydrated $NaBO_2^-$ and to cool the formed clusters. The cluster anions were mass-analyzed by the time-of-flight mass spectrometer. The $NaBO_2^-(H_2O)_n$ (n = 0–4) clusters were each mass-selected and decelerated before being photodetached. The electrons resulting from photodetachment were energy-analyzed by the magnetic-bottle photoelectron spectrometer. The photoelectron spectra were calibrated using the known spectrum of Cu^-. The instrumental resolution was approximately 40 meV for electrons with 1 eV kinetic energy.

2.2 Computational methods

The Gaussian09[41] program package was used for all the calculations. The structures of $NaBO_2^-(H_2O)_n$ (n = 0–4) clusters and their neutrals were first optimized with density functional theory employing the B3LYP[42,43] functional and 6-311+G** basis set. Then, more accurate energies of the structures were obtained by single-point calculations using the CCSD[44–46] method and aug-cc-pvtz basis set except that the single-point energies of $NaBO_2(H_2O)_4$ anion and neutral were calculated using CCSD method and aug-cc-pvdz basis set. No symmetry constraint was employed during the optimizations. The calculated energies were corrected by the zero-point vibrational energies. Harmonic vibrational frequencies were calculated to make sure that the structures corresponded to real local minima.

3. Experimental results

3.1 Mass spectra

Fig. 1 shows a typical mass spectrum of cluster anions generated in the experiments. It can be seen that the major mass peaks are those of $NaBO_2^-(H_2O)_n$ cluster anions and BO_2^-. The assignments of the mass peaks were confirmed by isotope abundance analysis as boron has two main isotopes, ^{10}B and ^{11}B with nature abundances of 19.9% and 80.1%, respectively. We are able to detect the mass peaks of $NaBO_2^-(H_2O)_n$ cluster anions up to n = 5. The mass signal of $NaBO_2^-(H_2O)_5$ is too low for taking a photoelectron spectrum. Thus, the photoelectron spectrum of $NaBO_2^-(H_2O)_5$ is not reported in this work.

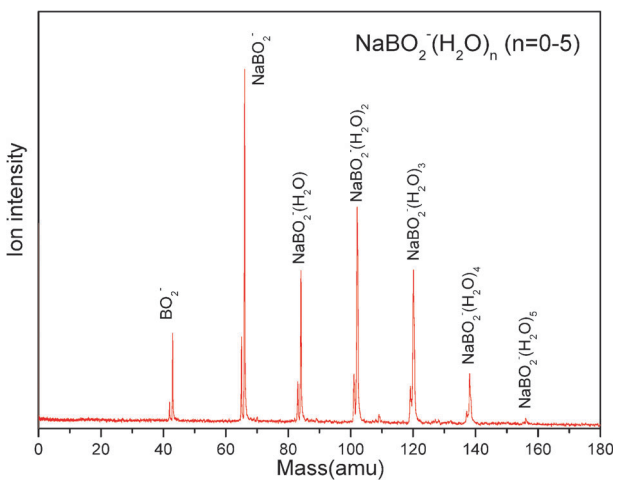

Fig. 1 Mass spectrum of $NaBO_2^-(H_2O)_n$ cluster anions.

3.2 Photoelectron spectra of $NaBO_2^-(H_2O)_n$ (n = 0–4)

The photoelectron spectra of $NaBO_2^-(H_2O)_n$ (n = 0–4) recorded with 532 nm photons are presented in Fig. 2. We also acquired the spectrum of $NaBO_2^-$ with 193 nm photons and the spectra of $NaBO_2^-(H_2O)_n$ (n = 0–2) with 266 nm photons, but no additional feature has been observed in these spectra at higher binding energies beyond the features observed in the 532 nm spectra. Thus, only the spectra taken with 532 nm photons are presented here. The vertical detachment energies (VDEs) and the adiabatic detachment energies (ADEs) of the $NaBO_2^-(H_2O)_n$ clusters estimated from their photoelectron spectra are summarized in Table 1. To account

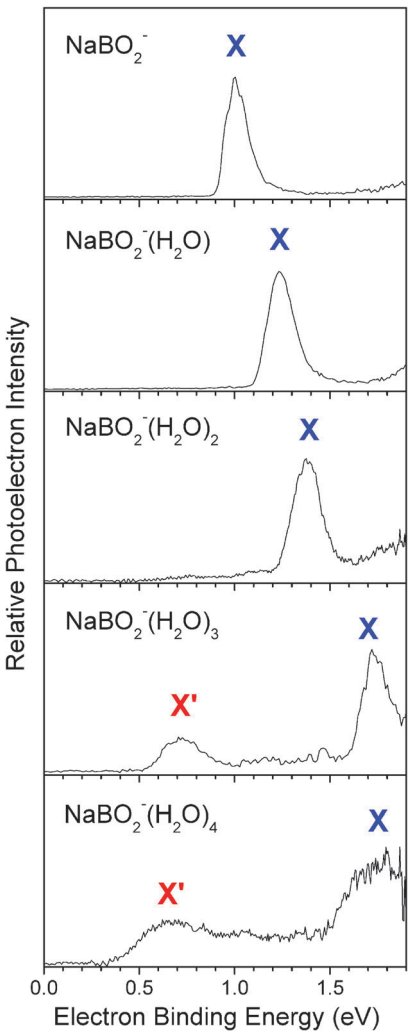

Fig. 2 Photoelectron spectra of $NaBO_2^-(H_2O)_n$ (n = 0–4) clusters recorded with 532 nm photons. The peaks labeled with X are from the Na–$BO_2^-(H_2O)_n$ type isomers. The peaks labeled with X′ are from the $Na(H_2O)_n\cdots BO_2^-$ type isomers.

Table 1 Experimentally observed VDEs and ADEs of $NaBO_2^-(H_2O)_n$ (n = 0–4) from their photoelectron spectra

	X′		X	
Cluster	ADE (eV)	VDE (eV)	ADE (eV)	VDE (eV)
$NaBO_2^-$			0.95 (±0.08)	1.00 (±0.08)
$NaBO_2^-(H_2O)$			1.14 (±0.08)	1.23 (±0.08)
$NaBO_2^-(H_2O)_2$			1.26 (±0.08)	1.38 (±0.08)
$NaBO_2^-(H_2O)_3$	0.59 (±0.15)	0.71 (±0.15)	1.66 (±0.08)	1.72 (±0.08)
$NaBO_2^-(H_2O)_4$	0.43 (±0.15)	0.65 (±0.15)	1.56 (±0.15)	1.76 (±0.15)

for the broadening of the photoelectron spectrum peaks due to instrumental resolution, the ADE was calculated by adding instrumental resolution to the onset of the first peak in the spectrum. The onset of the first peak was determined by drawing a straight line along the leading edge of that peak to cross the baseline of the spectrum.

In Fig. 2, we can see that the photoelectron spectrum of $NaBO_2^-$ shows a strong peak centered at 1.00 eV. The VDE and ADE of $NaBO_2$ are estimated to be 1.00 and 0.95 eV respectively based on the spectrum. As mentioned earlier, the spectrum of $NaBO_2^-$ taken with 193 nm photons shows no additional peaks, indicating the binding energy of the second peak is higher than the 193 nm photon energy (6.424 eV). That means that neutral $NaBO_2$ has a very large HOMO–LUMO gap (>5.4 eV). The spectra of $NaBO_2^-(H_2O)$ and $NaBO_2^-(H_2O)_2$ are very similar to that of $NaBO_2^-$, except that the peak of $NaBO_2^-(H_2O)$ shifts to a high EBE by 0.23 eV and that of $NaBO_2^-(H_2O)_2$ shifts to a high EBE by 0.38 eV. This phenomenon indicates that $NaBO_2^-$ is dissolved by water molecules and its electronic feature shifts due to the solvation effect.

The photoelectron spectra of $NaBO_2^-(H_2O)_3$ and $NaBO_2^-(H_2O)_4$ are quite different from those of $NaBO_2^-(H_2O)_{0-2}$. A broad feature centered at 0.71 eV (labeled with X′) and a dominating strong peak centered at 1.72 eV (labeled with X) are observed for $NaBO_2^-(H_2O)_3$. Similarly, two major features centered at 0.65 eV (X′) and 1.76 eV (X) are evident in the photoelectron spectrum of $NaBO_2^-(H_2O)_4$. The second peaks (X) in the spectra of $NaBO_2^-(H_2O)_3$ and $NaBO_2^-(H_2O)_4$ are similar to that of $NaBO_2^-$. They shift toward a higher EBE due to the addition of water molecules. We suggest that the emergence of the low binding feature (X′) is due to the separation of Na and BO_2^- by the water molecules. The details will be discussed later.

4. Theoretical results and discussion

The optimized geometries of the low-lying isomers of $NaBO_2^-(H_2O)_n$ (n = 0–4) clusters and their neutral counterparts obtained by theoretical calculations are presented in Fig. 3 and 4 with the most stable structures on the left. The calculated VDEs and ADEs of $NaBO_2^-(H_2O)_n$ (n = 0–4) clusters are listed in Table 2 along with the experimental VDEs and ADEs. The theoretical adiabatic electron detachment energies (ADEs) were calculated as the energy differences between the anions and the neutral counterparts relaxed to the nearest local minima from the geometries of the anions. The single-point energies used to determine the ADEs and VDEs were corrected by the zero-point vibrational energies. We have also simulated photoelectron spectra of the isomers of $NaBO_2^-(H_2O)_n$ (n = 0–4). The simulations were conducted by first calculating the electronic excited states of the neutrals at the geometries of the corresponding cluster ions by the CIS method[47] with the 6-311+G** basis set. The VDEs of the transitions from the ground state of the anion to the ground and excited states of the neutral were determined based on their relative energies to the ground state of the anion. The transitions were then fitted with Gaussian functions of 0.2 eV width to generate the simulated spectra. The purpose of the simulated spectra is to show the positions of the electronic transitions, the vibrational structures are not included. The simulated spectra of $NaBO_2^-(H_2O)_n$ (n = 0–4) are presented in Fig. 5.

4.1 $NaBO_2^-$ and $NaBO_2$

The most stable structure of $NaBO_2^-$ (0A) is a linear structure with the Na atom attached to one end of O═B═O. Similar to what we observed in $FeBO_2^-$,[35] the structure of the BO_2 unit and the B–O bond length in $NaBO_2^-$ are nearly identical to those in the bare BO_2^-. The theoretical ADE and VDE of isomer 0A are in agreement with the experiment values. The second and third isomers (0B and 0C) are less stable than isomer 0A by ~4 eV. Their theoretical ADEs and VDEs are very different from our experimental measurements. Thus, the existence of isomer 0B and 0C can be excluded. Isomer 0A is what we observed in the experiments.

Our calculations show that the ground state geometry of neutral $NaBO_2$ is also linear with slightly shorter Na–(OBO) distance than that in the anion. That is consistent with previous theoretical calculations.[48] That the Na–O bond in neutral $NaBO_2$ is shorter than that in $NaBO_2^-$ is probably due to the Coulomb interaction between the Na^+–(BO_2^-) ion pair. The Mulliken population analysis of neutral $NaBO_2$ shows that the charge of Na is positive while that of BO_2 is negative with the distribution of $(Na)^{0.946+}(OBO)^{0.946-}$. That is similar to the charge distributions of alkali halides. In addition, the $NaBO_2$ neutral cluster has a fairly large dipole moment of 13.1 D, which is comparable to those of typical ionic compounds, such as NaCl (9.0 D), KCl (10.3 D), NaBr (9.1 D), and KBr (10.6 D). When an excess electron is added to $NaBO_2$ to form an anion, the excess electron mainly localizes on the positive pole of the dipole, which is also similar to the case of halogen salts.

According to the simulated spectrum of $NaBO_2^-$ in Fig. 5, the second photoelectron spectral peak of $NaBO_2^-$ is centered at ~7.2 eV, beyond the range of 193 nm photons. That is consistent with the non-observation of the second peak in

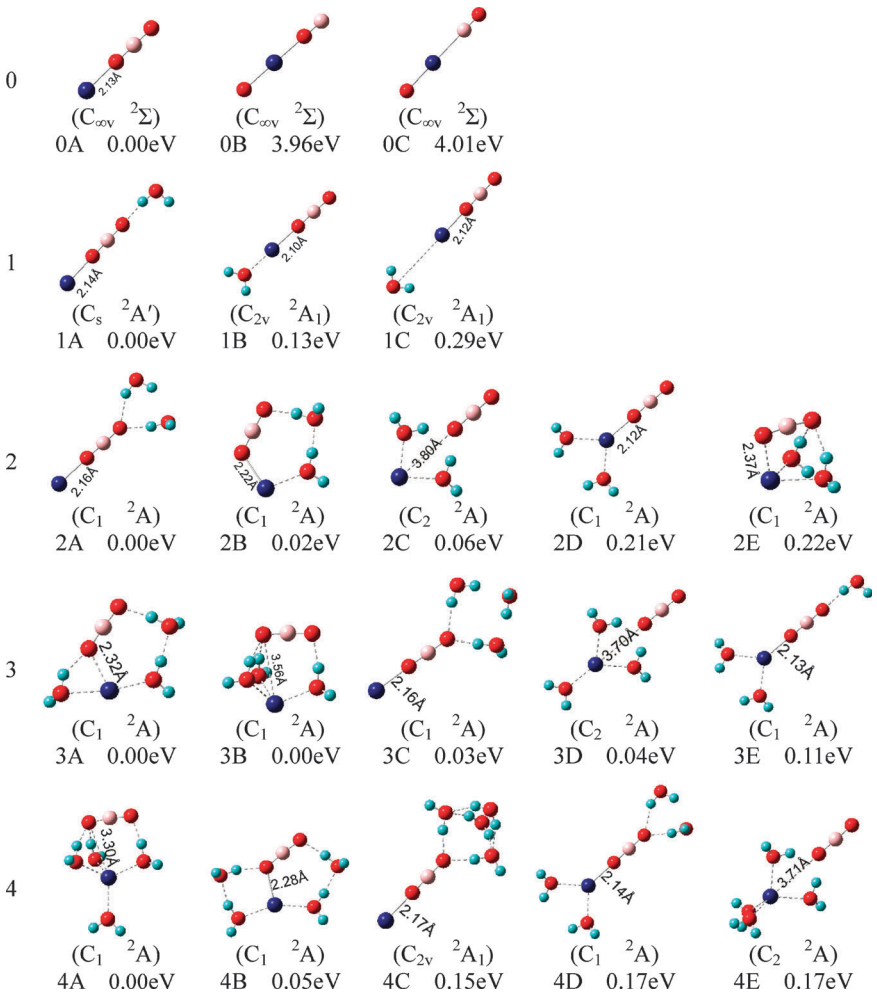

Fig. 3 Optimized geometries of the typical low-lying isomers of $NaBO_2^-(H_2O)_n$ (n = 0–4).

our experiments. It is also in agreement with the large HOMO–LUMO gap of $NaBO_2$ neutral.

4.2 $NaBO_2^-(H_2O)_1$ and $NaBO_2(H_2O)_1$

The lowest energy geometry of $NaBO_2^-(H_2O)_1$ (isomer 1A) has C_s symmetry with the water forming hydrogen bond with the terminal oxygen of $NaBO_2^-$. The theoretical VDE (1.16 eV) and ADE (1.10 eV) of isomer 1A are both close to the experimental VDE (1.23 eV) and ADE (1.14 eV). Isomer 1B has C_{2v} symmetry with the O atom of the water molecule connected to the Na atom. It is less stable than isomer 1A by only 0.13 eV. However, its VDE is much different from the experimental value. Isomer 1C is higher than isomer 1A by 0.29 eV, it also has C_{2v} symmetry but with opposite orientation of water molecule compared to that in isomer 1B. The calculated VDE and ADE of isomer 1C deviate from the experimental values. That implies that isomer 1A is dominating in the experiments.

The ground state geometry of neutral $NaBO_2(H_2O)_1$ is different from that of the anion. It has one of the water O–H bonds approaching the Na–O bond of $NaBO_2$. That probably is because the positively charged Na attracts the O atom of water while the negatively charged O attracts the H atom of water. The Na–O–B angle is bent as a consequence of the interaction between the Na–O and O–H bonds.

4.3 $NaBO_2^-(H_2O)_2$ and $NaBO_2(H_2O)_2$

The first three isomers of $NaBO_2^-(H_2O)_2$ (2A, 2B, and 2C) are nearly degenerate in energy. Isomer 2A is formed by addition of two water molecules to the terminal oxygen of $NaBO_2^-$. Both water molecules form hydrogen bonds with the terminal oxygen. The calculated VDE and ADE of isomer 2A are 1.24 and 1.22 eV, respectively, in agreement with the experiment values (1.38 and 1.26 eV). Isomer 2B has the two water molecules bridging the Na atom and the terminal O atom of $NaBO_2$. It can be considered as a ring formed by OBO, Na, and two H_2O. The Na–O–B angle is bent, and the Na–O bond of $NaBO_2^-$ increases from 2.13 Å to 2.22 Å. The calculated VDE and ADE of isomer 2B are different from the binding energy of the major peak observed in the photoelectron spectrum of $NaBO_2^-(H_2O)_2$ (Fig. 2). Isomer 2C has the two H_2O molecules attaching to the waist of $NaBO_2$ with the O atom of water interacting with Na and the H atom of water interacting with O=B=O$^-$. The Na–(OBO) distance increases significantly to 3.80 Å due to the introducing of two water molecules between Na and the OBO unit. Isomer

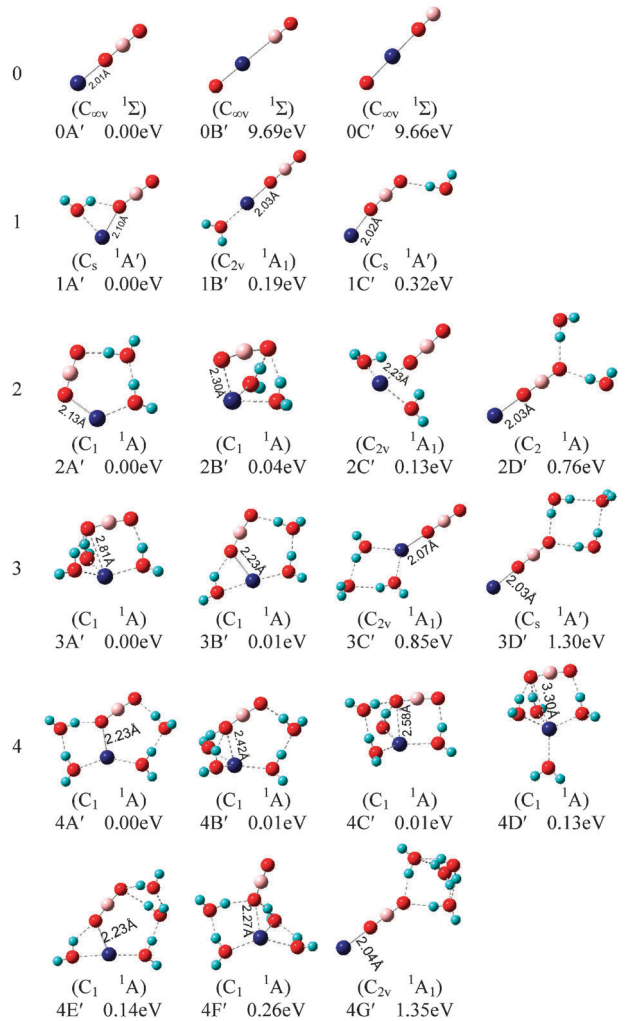

Fig. 4 Optimized geometries of the typical low-lying isomers of $NaBO_2(H_2O)_n$ (n = 0–4) neutral clusters.

2D is less stable than isomer 2A by 0.21 eV. In isomer 2D, the water molecules interact with $NaBO_2$ from the Na atom side, thus, do not have much effect on the Na–(OBO) distance. Isomer 2E is less stable than isomer 2A by 0.22 eV. It has both water molecules interacting with the Na atom and the terminal O atom of $NaBO_2$. The VDEs of isomer 2C and 2E are calculated to be 0.87 and 0.38 eV, respectively, much lower than the experimental value. The calculated VDE of isomer 2D (1.04 eV) is close to the experimental VDE, however, its ADE is much different. Based on the above analysis, we suggest that the major peak in the experimental photoelectron spectrum of $NaBO_2^-(H_2O)_2$ (Fig. 2) is contributed by isomer 2A. In the experimental spectrum of $NaBO_2^-(H_2O)_2$, there are some weak signals barely above the baseline in the range of 0.7–1.2 eV, implying that very small amounts of isomers 2B, 2C and 2D probably exist in the experiments.

The most stable structure of $NaBO_2(H_2O)_2$ neutral (2A′) is similar to that of isomer 2B. In isomer 2A′, the Na–O bond of $NaBO_2$ increases from 2.01 Å to 2.13 Å upon interacting with the water molecules. Isomer 2B′ is similar to isomer 2E of the anion with both water molecules interacting with the Na atom and the terminal O atom of $NaBO_2$. The structure of isomer 2C′ is similar to isomer 2C, being slightly bent in $NaBO_2$. It is less stable than isomer 2A′ by 0.13 eV. Since the effect of the water molecule on the Na–O bond is stronger in 2C′, its Na–(OBO) distance is longer than that of 2A′ by 0.1 Å. The energy of isomer 2D′ is 0.76 eV higher than that of isomers 2A′, indicating that attaching of the water molecule to the oxygen end of $NaBO_2$ is not favored in the neutral cluster.

Table 2 Relative energies of the low energy isomers of $NaBO_2^-(H_2O)_n$ (n = 0–4) as well as the comparison of their theoretical VDEs and ADEs to the experimental measurements. The isomers labeled in bold are the most probable isomers in the experiment

					ADE (eV)		VDE (eV)	
Isomer		ΔE^a (eV)	State	Sym.	Theo.	Exp.	Theo.	Exp.
$NaBO_2^-$	**0A**	0.00	$C_{\infty v}$	$^2\Sigma$	0.98	0.95	1.00	1.00
	0B	3.96	$C_{\infty v}$	$^2\Sigma$	6.71		6.79	
	0C	4.01	$C_{\infty v}$	$^2\Sigma$	6.63		6.65	
$NaBO_2^-(H_2O)$	**1A**	0.00	C_s	$^2A'$	1.10	1.14	1.16	1.23
	1B	0.13	C_{2v}	$^2A_1$	0.85		0.90	
	1C	0.29	C_{2v}	$^2A_1$	0.49		1.39	
$NaBO_2^-(H_2O)_2$	**2A**	0.00	C_1	^2A	1.22	1.26	1.24	1.38
	2B	0.02	C_1	^2A	0.43		0.51	
	2C	0.06	C_2	^2A	0.52		0.87	
	2D	0.21	C_1	^2A	0.37		1.04	
	2E	0.22	C_1	^2A	0.27		0.38	
$NaBO_2^-(H_2O)_3$	3A	0.00	C_1	^2A	0.22		0.36	
	3B	0.00	C_1	^2A	0.20		0.34	
	3C	0.03	C_1	^2A	1.47	1.66	1.63	1.72
	3D	0.04	C_2	^2A	0.18	0.59	0.82	0.71
	3E	0.11	C_1	^2A	0.11		1.18	
$NaBO_2^-(H_2O)_4$	**4A**	0.00	C_1	^2A	0.35	0.43	0.49	0.65
	4B	0.05	C_1	^2A	0.16		0.29	
	4C	0.15	C_{2v}	$^2A_1$	1.42	1.56	1.49	1.76
	4D	0.17	C_1	^2A	0.18		1.19	
	4E	0.17	C_2	^2A	0.31		0.99	

[a] The single-point energies of $NaBO_2^-(H_2O)_n$ (n = 0–3) were calculated using the CCSD method and aug-cc-pvtz basis set. The single-point energies of $NaBO_2^-(H_2O)_4$ were calculated using CCSD method and aug-cc-pvdz basis set. All energies were corrected by the zero-point vibrational energies.

4.4 $NaBO_2^-(H_2O)_3$ and $NaBO_2(H_2O)_3$

The first four isomers of $NaBO_2^-(H_2O)_3$ (3A, 3B, 3C, and 3D) are nearly degenerate in energy. 3A is derived from isomer 2B by attaching the third H_2O to the Na–O bond of $NaBO_2$. Isomer 3B has three water molecules sitting between the Na atom and the tilting OBO unit. The first two water molecules form hydrogen bonds with one end of the OBO unit while the third water molecule forms a hydrogen bond with the other end of the OBO unit. The O atoms of the three water molecules all interact with the Na atom. The Na–(OBO) distance in isomer 3B increases to 3.56 Å due to the strong interaction between the water molecules and Na–O bond of $NaBO_2$. Isomer 3C has three water molecules all located near the oxygen end of $NaBO_2$ with the first two H_2O molecules forming hydrogen bonds with the terminal O atom of $NaBO_2$ and the third H_2O bridging the first two H_2O molecules. The Na–(OBO) distance in isomer 3C is only slightly lengthened compared to that in bare $NaBO_2^-$. Isomer 3D can be considered as having evolved from isomer 2C of $NaBO_2^-(H_2O)_2$ by addition of the third H_2O to the Na atom. Consequently, the Na atom is surrounded by the three water molecules. The

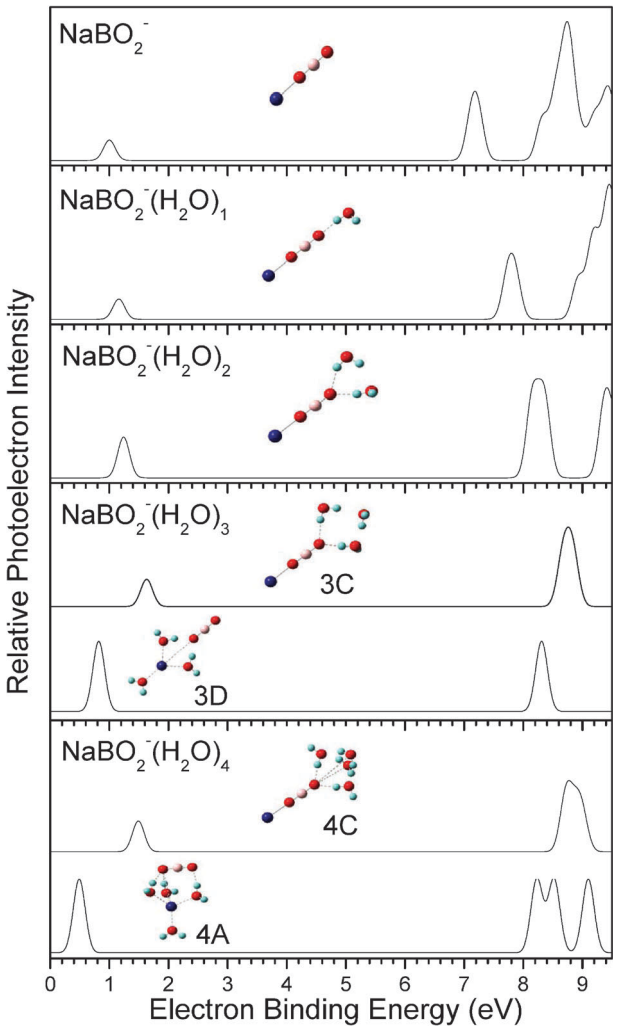

Fig. 5 Simulated spectra of the typical low-lying isomers of $NaBO_2^-(H_2O)_n$ (n = 0–4). The simulations indicate that the $NaBO_2(H_2O)_n$ neutrals have larger HOMO–LUMO gaps.

Na–(OBO) distance increases to 3.70 Å compared with the distance of 2.13 Å in bare $NaBO_2^-$. Isomer 3E is less stable than isomer 3A by 0.11 eV. It can be considered as having derived from isomer 2D of $NaBO_2^-(H_2O)_2$ by adding a water molecule to the oxygen end of $NaBO_2$. The calculated VDEs for the isomers from 3A to 3E are 0.36, 0.34, 1.63, 0.82 and 1.18 eV respectively. The VDE of isomer 3D is in agreement with the VDE of the low EBE peak in the spectrum of $NaBO_2^-(H_2O)_3$ (Fig. 2), and that of isomer 3C (1.63 eV) in agreement with the VDE of the high EBE peak (1.72 eV) in the spectrum. Thus, isomer 3D can be associated to the low EBE feature of $NaBO_2^-(H_2O)_3$ observed in our experiments, while isomer 3C can be associated to the high EBE peak in the experiments. As can be seen from Fig. 2, there are also some signals between the two major peaks. That probably is due to the small amount of isomer 3E in the experiments.

For neutral $NaBO_2(H_2O)_3$, the first two isomers (3A′ and 3B′) are nearly degenerate in energy. Isomer 3A′ is similar to isomer 3B, in which the Na^+/OBO^- ion pair is separated by the three H_2O molecules. The Na–(OBO) distance in isomer 3A′ is about 2.81 Å, longer than the length of 2.01 Å in bare $NaBO_2$. The structure of isomer 3B′ is obtained by attaching a H_2O molecule to the Na–O side of the ring of isomer 2A′. Isomer 3C′ is less stable than the lowest isomer (3A′) by 0.85 eV. It has all three water molecules located near the Na end of $NaBO_2$. Isomer 3D′ has all three water molecules located at the O end of $NaBO_2$. It is less stable than isomer 3A′ by 1.30 eV. That indicates that attaching of water molecules to the oxygen end of $NaBO_2$ is not favored in $NaBO_2(H_2O)_3$ either, in agreement with the case of neutral $NaBO_2(H_2O)_2$.

4.5 $NaBO_2^-(H_2O)_4$ and $NaBO_2(H_2O)_4$

Similar to the $NaBO_2^-(H_2O)_3$ cluster, there are several isomers of $NaBO_2^-(H_2O)_4$ coexisting in the experiments. Isomers 4A and 4B are nearly degenerate in energy. In isomer 4A, the Na atom is surrounded by four water molecules. Three of the water molecules sit between the Na and OBO unit. The OBO unit tilts due to the interaction with three water molecules. Isomer 4B is evolved from isomer 3A by attaching the second H_2O to the Na–O side. The Na–(OBO) distances in isomers 4A and 4B are both larger than that in bare $NaBO_2^-$. The theoretical VDEs of isomers 4A and 4B are 0.49 and 0.29 eV respectively. The VDE of isomer 4A is consistent with the broad low EBE feature labeled with X′) (Fig. 2). Isomer 4C has all four water molecules at the terminal O atom side. The calculated VDE (1.49 eV) of isomer 4C is in reasonable agreement with the VDE of the high EBE peak (labeled with X) in the photoelectron spectrum of $NaBO_2^-(H_2O)_4$ (Fig. 2). Here, the calculated VDE of isomer 4C is even lower than that of isomer 3C, probably due to the difference of basis sets used for calculation. Isomers 4D and 4E are degenerate in energy and higher than isomer 4A by 0.17 eV respectively. Isomer 4D has two water molecules at the Na side and the other two molecules at the terminal O side of $NaBO_2$. The calculated VDE of isomer 4D is 1.19 eV, lower than the VDE of the high EBE peak by 0.57 eV. Isomer 4E is derived from isomer 3D by adding the fourth H_2O to the Na atom. The Na–(OBO) distance in isomer 4E is about 3.71 Å. The theoretical VDE of isomer 4E is calculated to be 0.99 eV, higher than the low EBE feature in the spectrum. We suggest that isomer 4A might be the major one that contributes to the low EBE feature in the spectrum. The high EBE feature in the spectrum of $NaBO_2^-(H_2O)_4$ can be assigned to isomer 4C. In the spectrum of $NaBO_2^-(H_2O)_4$, some photoelectron signals can also be observed between those two major peaks. That probably can be attributed to the presence of a small amount of isomers 4D and 4E as their VDEs fall into that region.

The low-lying isomers of neutral $NaBO_2(H_2O)_4$ are also close in energy. Isomers 4B′ and 4C′ are higher than isomer 4A′ by only 0.01 eV. Isomers 4A′ and 4B′ are evolved from isomer 3B′. They are also similar to anionic isomer 4B. Both isomers 4C′ and 4D′ can be considered as derived from isomer 3A′. Isomer 4E′ is in the same category of isomers 4A′ and 4B′ except its fourth water molecule binds to the terminal O atom of $NaBO_2$. In isomer 4F′, all the four H_2O molecules interact with the Na–O bond of $NaBO_2$. We have also tried the structure with all four H_2O molecules located near the terminal O atom of $NaBO_2$ (Isomer 4G′) and found it is less stable than the lowest structure by 1.35 eV.

Fig. 5 shows that the simulated spectrum of isomer 3C coordinates nicely to the 1.72 eV feature of $NaBO_2^-(H_2O)_3$ in the experiments, that of isomer 3D matches up the low EBE feature of $NaBO_2^-(H_2O)_3$. Similarly, the simulated spectrum of isomer 4C is consistent with the 1.76 eV feature of $NaBO_2^-(H_2O)_4$, while that of isomer 4A is in agreement with the low EBE feature of $NaBO_2^-(H_2O)_4$.

Overall, we can divide the structures of $NaBO_2^-(H_2O)_n$ into two types, $Na–BO_2^-(H_2O)_n$ and $Na(H_2O)_n\cdots BO_2^-$. The most stable structures of $NaBO_2^-(H_2O)$ and $NaBO_2^-(H_2O)_2$ are the $Na–BO_2^-(H_2O)_n$ type in which the water molecules prefer to form hydrogen bonds with the terminal oxygen of $NaBO_2$. For $NaBO_2^-(H_2O)_3$ and $NaBO_2^-(H_2O)_4$, the $Na–BO_2^-(H_2O)_n$ and $Na(H_2O)_n\cdots BO_2^-$ types coexist because they are close in energy. The lowest structures of $NaBO_2^-(H_2O)_3$ and $NaBO_2^-(H_2O)_4$ are the $Na(H_2O)_n\cdots BO_2^-$ type in which the H_2O molecules bond to the Na atom which is favorable. The high EBE features in the photoelectron spectrum of $NaBO_2^-(H_2O)_n$ (n = 1–4) are attributed to the $Na–BO_2^-(H_2O)_n$ type of isomers, such as 1A, 2A, 3C, and 4C. In the $Na–BO_2^-(H_2O)_n$ type of isomers, the water molecules interact with the terminal oxygen of BO_2^-. The Na–(OBO) bond is only slightly affected by addition of water molecules. The structure of $NaBO_2^-$ unit is almost unchanged. Thus, the photoelectron spectral features of isomers 1A, 2A, 3C, and 4C are similar to that of bare $NaBO_2^-$ except they shift toward high EBEs due to the solvation effect of the water molecules. That is quite similar to the solvation effect in some other systems, such as $X^-(H_2O)_n$ (X = Cl, Br and I).[49] The low EBE features in the photoelectron spectrum of $NaBO_2^-(H_2O)_3$ and $NaBO_2^-(H_2O)_4$ can be attributed to the $Na(H_2O)_n\cdots BO_2^-$ type of isomers where the water molecules interact strongly with the Na atom and BO_2^-, the Na–(OBO) bond is lengthened significantly, and the structure of $NaBO_2^-$ is bent. For the photodetachment of the $Na(H_2O)_n\cdots BO_2^-$ type of isomers, the local environment of the initial state is H_2O solvating the neutral Na atom while that of the final state is water solvating the Na^+ cation. The strong interaction between H_2O and Na^+ cation stabilizes the final state (reduces the energy of the final state), thus, the electron binding energy of the $Na(H_2O)_n\cdots BO_2^-$ type of isomers is even lower than that of the bare $NaBO_2^-$, giving rise to the X′ low binding energy features for n = 3 and 4.

In neutral $NaBO_2(H_2O)_n$, the water molecules prefer to interact with the Na^+ end (including the Na–O bond) rather than the terminal oxygen of BO_2^-. That probably is because the Na is positively charged and the oxygen of water molecule has lone pair electrons. Thus, the water molecules can stabilize the clusters by sharing the lone pair electrons of its O atom with the Na^+ ion. In some cases, the H atoms of the water molecules may interact with the O atom of BO_2 unit near the Na^+ end. The structures, such as isomers 1C′, 2D′, 3D′ and 4G′, with all H_2O near the terminal oxygen are relatively unstable. That is consistent with what is found in the $NaCl(H_2O)_n$ systems where the Na^+–(H_2O) interaction is stronger than the Cl^-–(H_2O) interaction.[11] It is also worth mentioning that, in the $NaBO_2^-(H_2O)_n$ cluster anions, the interaction between the water molecules and sodium atom becomes stronger when the cluster size increases. Thus, the most stable structures of $NaBO_2^-(H_2O)_n$ anions become more similar to those of their corresponding neutral clusters with increasing number of water molecules.

5. Conclusions

We investigated $NaBO_2^-(H_2O)_n$ cluster anions with mass spectrometry and photoelectron spectroscopy. The photoelectron spectra of $NaBO_2^-(H_2O)_1$ and $NaBO_2^-(H_2O)_2$ are similar to that of bare $NaBO_2^-$, except that their VDEs shift to higher electron binding energies. Starting from $NaBO_2^-(H_2O)_3$, a dramatic change in the photoelectron spectra shows up. In the spectra of $NaBO_2^-(H_2O)_3$ and $NaBO_2^-(H_2O)_4$, a low EBE feature shows up in addition to the similar feature observed in the spectra of $NaBO_2^-(H_2O)_{0–2}$, indicating that the $Na–BO_2^-(H_2O)_n$ and $Na(H_2O)_n\cdots BO_2^-$ type structures coexist, the water molecules start to separate Na and BO_2^- to form SSIP type structures in $NaBO_2^-(H_2O)_3$ and $NaBO_2^-(H_2O)_4$ clusters. The results of theoretical calculations are in agreement with the experiments. We also found that the most stable structures of $NaBO_2^-(H_2O)_n$ anions are different from their corresponding neutral structures at small cluster size, but become more similar to the neutral structures as cluster size increases.

Acknowledgements

WJZ acknowledges the Institute of Chemistry, Chinese Academy of Sciences for start-up funds. We are grateful to Professor Zhen Gao for valuable discussions. The theoretical calculations were conducted on the ScGrid and Deepcomp7000 of the Supercomputing Center, Computer Network Information Center of the Chinese Academy of Sciences.

References

1 M. P. Apse, G. S. Aharon, W. A. Snedden and E. Blumwald, *Science*, 1999, **285**, 1256.
2 P. Neysens, W. Messens and L. De Vuyst, *Int. J. Food Microbiol.*, 2003, **88**, 29.
3 T. Cserháti and E. Forgács, *Int. J. Pharm.*, 2003, **254**, 189.
4 C. K. Siu, B. S. Fox-Beyer, M. K. Beyer and V. E. Bondybey, *Chem.–Eur. J.*, 2006, **12**, 6382.
5 E. E. Gard, M. J. Kleeman, D. S. Gross, L. S. Hughes and J. O. Allen, *et al.*, *Science*, 1998, **279**, 1184.
6 K. W. Oum, M. J. Lakin, D. O. DeHaan, T. Brauers and B. J. Finlayson-Pitts, *Science*, 1998, **279**, 74.
7 E. M. Knipping, M. J. Lakin, K. L. Foster, P. Jungwirth and D. J. Tobias, *et al.*, *Science*, 2000, **288**, 301.
8 B. J. Finlayson-Pitts, *Chem. Rev.*, 2003, **103**, 4801.
9 L. E. de-Bashan and Y. Bashan, *Water Res.*, 2004, **38**, 4222.
10 N. Tsipouras, C. J. Rix and P. H. Brady, *Clin. Chem.*, 1997, **43**, 290.
11 D. E. Woon and T. H. Dunning, *J. Am. Chem. Soc.*, 1995, **117**, 1090.
12 G. H. Peslherbe, B. M. Ladanyi and J. T. Hynes, *J. Phys. Chem. A*, 1998, **102**, 4100.
13 C. P. Petersen and M. S. Gordon, *J. Phys. Chem. A*, 1999, **103**, 4162.
14 G. H. Peslherbe, B. M. Ladanyi and J. T. Hynes, *J. Phys. Chem. A*, 2000, **104**, 4533.
15 G. H. Peslherbe, B. M. Ladanyi and J. T. Hynes, *Chem. Phys.*, 2000, **258**, 201.
16 P. Jungwirth, *J. Phys. Chem. A*, 2000, **104**, 145.
17 S. Yamabe, H. Kouno and K. Matsumura, *J. Phys. Chem. B*, 2000, **104**, 10242.

18 P. Jungwirth and D. J. Tobias, *J. Phys. Chem. B*, 2001, **105**, 10468.
19 S. Godinho, P. C. do Couto and B. J. C. Cabral, *Chem. Phys. Lett.*, 2006, **419**, 340.
20 A. C. Olleta, H. M. Lee and K. S. Kim, *J. Chem. Phys.*, 2006, **124**, 024321.
21 A. C. Olleta, H. M. Lee and K. S. Kim, *J. Chem. Phys.*, 2007, **126**, 144311.
22 G. Sciaini, R. Fernandez-Prini, D. A. Estrin and E. Marceca, *J. Chem. Phys.*, 2007, **126**, 174504.
23 B. S. Ault, *J. Am. Chem. Soc.*, 1978, **100**, 2426.
24 G. Gregoire, M. Mons, C. Dedonder-Lardeux and C. Jouvet, *Eur. Phys. J. D*, 1998, **1**, 5.
25 G. Gregoire, M. Mons, I. Dimicoli, C. Dedonder-Lardeux and C. Jouvet, *et al.*, *J. Chem. Phys.*, 2000, **112**, 8794.
26 C. Dedonder-Lardeux, G. Gregoire, C. Jouvet, S. Martrenchard and D. Solgadi, *Chem. Rev.*, 2000, **100**, 4023.
27 X. B. Wang, C. F. Ding, J. B. Nicholas, D. A. Dixon and L. S. Wang, *J. Phys. Chem. A*, 1999, **103**, 3423.
28 J. J. Max and C. Chapados, *J. Chem. Phys.*, 2001, **115**, 2664.
29 Q. Zhang, C. J. Carpenter, P. R. Kemper and M. T. Bowers, *J. Am. Chem. Soc.*, 2003, **125**, 3341.
30 A. Mizoguchi, Y. Ohshima and Y. Endo, *J. Am. Chem. Soc.*, 2003, **125**, 1716.
31 A. T. Blades, M. Peschke, U. H. Verkerk and P. Kebarle, *J. Am. Chem. Soc.*, 2004, **126**, 11995.
32 M. J. Blandame, *Chem. Rev.*, 1970, **70**, 59.
33 X.-B. Wang, H.-K. Woo, B. Jagoda-Cwiklik, P. Jungwirth and L.-S. Wang, *Phys. Chem. Chem. Phys.*, 2006, **8**, 4294.
34 Y. Kojima, *R& D Review of Toyota CRDL*, 2005, **40**, 31.
35 Y. Feng, H.-G. Xu, Z.-G. Zhang, Z. Gao and W.-J. Zheng, *J. Chem. Phys.*, 2010, **132**, 074308.
36 M. Götz, M. Willis, A. K. Kandalam, G. F. Ganteför and P. Jena, *ChemPhysChem*, 2010, **11**, 853.
37 M. Willis, M. Götz, A. K. Kandalam, G. F. Ganteför and P. Jena, *Angew. Chem., Int. Ed.*, 2010, **49**, 8966.
38 Y. Feng, H.-G. Xu, W. J. Zheng, H. M. Zhao and A. K. Kandalam, *et al.*, *J. Chem. Phys.*, 2011, **134**, 094309.
39 G. L. Gutsev and A. I. Boldyrev, *Chem. Phys.*, 1981, **56**, 277.
40 H.-G. Xu, Z.-G. Zhang, Y. Feng, J. Y. Yuan and Y. C. Zhao, *et al.*, *Chem. Phys. Lett.*, 2010, **487**, 204.
41 M. J. Frisch, G. W. Trucks and H. B. Schlegel *et al.*, *Gaussian 09*, Gaussian Inc.,Wallingford CT, 2009.
42 A. D. Becke, *J. Chem. Phys.*, 1993, **98**, 5648.
43 C. T. Lee, W. T. Yang and R. G. Parr, *Phys. Rev. B*, 1988, **37**, 785.
44 G. D. Purvis and R. J. Bartlett, *J. Chem. Phys.*, 1982, **76**, 1910.
45 G. E. Scuseria, C. L. Janssen and H. F. Schaefer, *J. Chem. Phys.*, 1988, **89**, 7382.
46 G. E. Scuseria and H. F. Schaefer, *J. Chem. Phys.*, 1989, **90**, 3700.
47 J. B. Foresman, M. Head-Gordon, J. A. Pople and M. J. Frisch, *J. Phys. Chem.*, 1992, **96**, 135.
48 F. Ramondo, L. Bencivenni and C. Sadun, *THEOCHEM*, 1990, **209**, 101.
49 G. Markovich, S. Pollack, R. Giniger and O. Cheshnovsky, *J. Chem. Phys.*, 1994, **101**, 9344.

